



ISSN: 2447-3359

REVISTA DE GEOCIÊNCIAS DO NORDESTE

Northeast Geosciences Journal

v. 10, nº 1 (2024)

<https://doi.org/10.21680/2447-3359.2024v10n1ID33855>



Mapping of land use and occupation in the Timbaúbas stream's micro-watershed in Juazeiro do Norte-CE using GIS

Mapeamento do uso e ocupação do solo da microbacia hidrográfica do Riacho Timbaúbas em Juazeiro do Norte-CE utilizando SIG

Maísa de Calda Lopes¹; Klinsmann Bezerra Rabelo²; Vinícius Alves Pereira da Luz³; Celme Torres Ferreira da Costa⁴; Ana Patrícia Nunes Bandeira⁵; Paulo Roberto Lacerda Taveres⁶

- ¹ Federal University of Ceará, Department of hydraulic and environmental engineering, Fortaleza-CE, Brasil. Address: maisa.lobes@alu.ufc.br
ORCID: <https://orcid.org/0009-0009-4950-828X>
- ² Federal University of Cariri, Civil Engineering Course, Juazeiro do Norte-CE, Brasil. Address: klinsmann.rabelo@aluno.ufca.edu.br
ORCID: <https://orcid.org/0009-0008-0048-6801>
- ³ Federal University, Civil Engineering Course, Juazeiro do Norte-CE, Brasil. Address: vinicius_apereira@hotmail.com
ORCID: <https://orcid.org/0000-0002-6819-4716>
- ⁴ Federal University, Civil Engineering Course, Juazeiro do Norte-CE, Brasil. Address celme.torres@ufca.edu.br
ORCID: <https://orcid.org/0000-0002-5368-5862>
- ⁵ Federal University, Civil Engineering Course, Juazeiro do Norte-CE, Brasil. Address: ana.bandeira@ufca.edu.br
ORCID: <https://orcid.org/0000-0001-7883-2796>
- ⁶ Federal University, Civil Engineering Course, Juazeiro do Norte-CE, Brasil. Address: paulo.tavares@ufca.edu.br
ORCID: <https://orcid.org/0000-0002-6702-7975>

Abstract: This article was developed in the watershed where Timbaúbas Park is located, an area designated as an Internal Full Protection Conservation Unit within the city of Juazeiro do Norte-CE. The main objective was to map land use and occupation, contributing to the analysis of precipitation on a macro-drainage scale. The delimitation of the watershed was conducted using the Haster Shuttle Radar Topography Mission (SRTM) image, and the CBERS 4A satellite image was used for the mapping of land use and occupation. Seven land use classes were identified: impervious areas (29.55%), water bodies (0.16%), dense vegetation (13.47%), vacant lands (19.97%), livestock (21.23%), agriculture (2.86%), and exposed soil (12.76%). The land use and occupation map presented satisfactory and coherent results, as its validation yielded an error matrix with a Kappa coefficient value of 0.84, indicating excellent performance, and a global accuracy of 87.59%. The study provided a detailed and accurate mapping of land use and occupation in the Timbaúbas Park watershed. The results are crucial for understanding the influence of land use in macro-drainage management and sustainable urban planning in the region.

Keywords: Land use and land cover; Mapping; GIS.

Resumo: O presente artigo foi desenvolvido na bacia hidrográfica na qual Parque Timbaúbas, área definida como Unidade de Conservação de Proteção Integral interna à cidade de Juazeiro do Norte-CE. O objetivo principal foi mapear o uso e a ocupação do solo, contribuindo para a análise da precipitação em escala de macrodrenagem. Para a delimitação da bacia hidrográfica foi utilizada a imagem *Haster Shuttle Radar Topography Mission* (SRTM) e para o mapeamento de uso e ocupação do solo foi utilizado a imagem do satélite CBERS 4ª. Foram identificadas sete classes de uso do solo: áreas impermeáveis (29,55%), corpos d'água (0,16%), vegetação densa (13,47%), terrenos baldios (19,97%), pastagens (21,23%), áreas cultivadas (2,86%) e solo exposto (12,76%). O mapa de uso e ocupação do solo apresentou resultados satisfatórios e coerentes, pois na sua validação foi obtida a matriz de erros, o valor do coeficiente *Kappa* de 0,84, indicando um excelente desempenho, acurácia global de 87,59%. O estudo proporcionou um mapeamento detalhado e preciso do uso e ocupação do solo na bacia hidrográfica do Parque Timbaúbas. Os resultados são fundamentais para compreender a influência do uso do solo na gestão da macrodrenagem e no planejamento urbano sustentável da região.

Palavras-chave: Uso e ocupação do solo; Mapeamento; SIG.

Received: 06/09/2024; Accepted: 01/12/2023; Published: 31/01/2024.

1. Introduction

As described by Silva and Silva (2017), the delimitation of land, coupled with the analysis of its use and occupation, within its carrying capacity, is crucial for socioeconomic planning of agricultural, industrial, and environmental activities. Furthermore, as stated by Santos *et al.* (2016), the disorganized occupation of urban space, a reality in many cities in Brazil, contributes to the emergence of risk areas, causing impacts on watersheds that often result in mass movements, erosive processes, floods, and inundations. In this context, as advocated by Alexandre *et al.* (2016a), the survey and mapping of land use are essential for understanding spatial organization patterns.

The development of new remote sensing and cartography techniques has been growing over the past decades, driven by the need to efficiently obtain data in terms of precision and short time frames from the environment (LIMA, SOUZA; 2016). As described by Fitz (2013), remote sensing can be defined as the technique capable of acquiring data without direct contact with the target, through electromagnetic radiation reflected by the surface components. These reflections are captured by orbital sensors, allowing the identification of each object and its level of reflectance based on the length of the waves. According to Cruz and Galo (2005), remote sensing provides spectral responses recorded by sensors installed on ground, airborne, or orbital platforms, such as the CBERS 4 satellite.

As asserted by Alexandre *et al.* (2016a), remote sensing is the most suitable method for collecting the necessary data for mapping due to its ability to record land use in a short period. This tool is indispensable for mapping extensive, dense, and hard-to-reach regions, such as the Amazon rainforest. In updating cartographic data for this area, Caldeira *et al.* (2023) employed remote sensing and geoprocessing based on the digital elevation model extracted through Light Detection and Ranging (LiDAR). Alexandre *et al.* (2016b) utilized the tool for updating data related to the vegetation cover of the municipality of Iati, Pernambuco.

Alexandre *et al.* (2016a) argue that the use of remote sensing in the survey and mapping of land use is essential for understanding spatial organization patterns, as applied by Machado *et al.* (2022) in the coastal region of the State of Espírito Santo, by Silva *et al.* (2022) in the “Córrego do Grotão”, Capitólio – Minas Gerais, and by Guedes and Cestaro (2018) in the land cover of the Brazilian semiarid region. According to the authors, remote sensing is the most suitable method for collecting the necessary data for mapping due to its ability to record land use in a brief period. Silva e Silva (2017) further emphasizes the potential of this tool for analyzing changes in land use and occupation that have occurred over the years.

Juazeiro do Norte, located in the state of Ceará, exhibits unplanned urban development and a deficient urban drainage system. According to Pereira (2013), the municipality ranks fifth in terms of the most urbanized areas in the state, rendering it susceptible to various issues resulting from precipitation phenomena, as observed in the City Natural Park of Timbaúbas. However, numerous erosive features have been identified at the site (Bandeira *et al.*, 2021), exacerbated by improper land use and occupation, environmental degradation, inadequate planning of stormwater, and deficiencies in executed drainage structures.

In this context, the purpose of this work is to present the characteristics of land use and occupation in the micro-watershed of the Timbaúbas stream, located in the city of Juazeiro do Norte, Ceará. The area is designated as a Full Protection Unit, which should be preserved to allow for both the replenishment of underground aquifers and serve as a recreational space for the population. To achieve the objective of this study, remote sensing, and Geographic Information System (GIS) techniques were employed, using the QGIS software. Based on the results obtained from the land use and occupation mapping, it will be possible to feed models enabling the analysis of flooding conditions and precipitation patterns in a given region. As suggested by Sousa *et al.* (2016), this information can support planning proposals for watershed management.

2. Study Area

The study area refers to the micro-watershed of the Timbaúbas stream (Figure 1), with its chosen estuary point corresponding to the northernmost position of the Municipal Natural Park of Timbaúbas. In this work, it will be referred to as the Timbaúbas Park, located in the municipality of Juazeiro do Norte, Ceará, with UTM coordinates 9.201.215N and 466.231E (Figure 2).

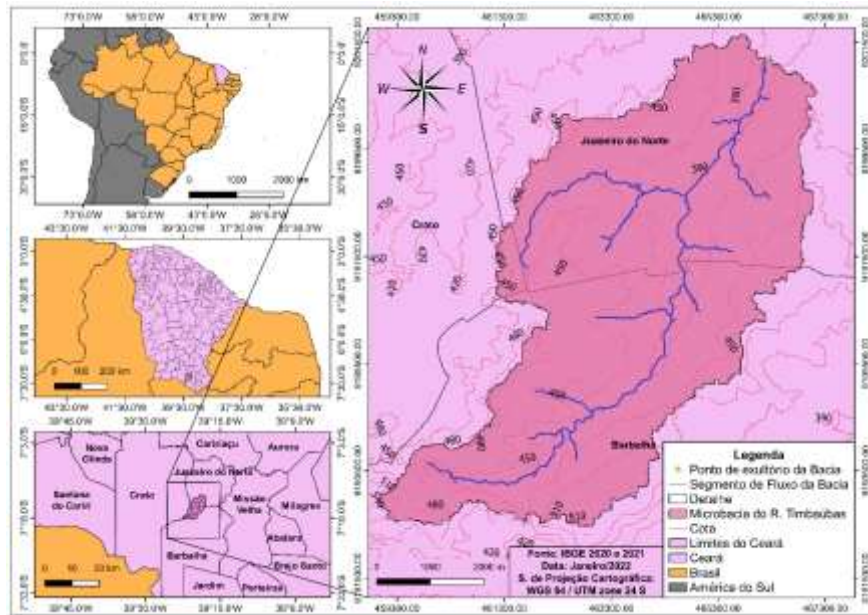


Figure 1 – Study Area Location Map
Source: Authors(2023)



Figure 2 – Location map of the estuary point in Timbaúbas Park. Source: authors
Source: Authors (2023)

Regarding vegetation cover, the municipality of Juazeiro do Norte, Ceará, exhibits typical semi-arid vegetation, deciduous forest. In terms of climatology, according to the Institute for Economic Research and Strategy of Ceará (IPECE, 2017), the municipality has an annual rainfall of 925.1 mm, with the rainy season concentrated from January to May, and an average temperature ranging from 24°C to 26°C.

Furthermore, concerning the location, as depicted in Figure 1, surface runoff originates from three cities: Barbalha, Crato, and Juazeiro do Norte. In the context of the analysis region, these cities have areas of 1,876.12 ha, 51.77 ha, and 1,807.28 ha, respectively. Thus, the micro-watershed encompasses a total area of 3,735.17 ha, a perimeter of 45.39 km, and a main flow length of 13.58 km.

3. Methodology

3.1 Acquisition of satellite images

Initially, the watershed in which the study area is located was delineated. For this purpose, a Shuttle Radar Topography Mission (SRTM) Haster image was used, which provides digital elevation data with a spatial resolution of 30m. The image was acquired from the Earth Explore United States Geological Survey (USGS) website.

For land use and land cover mapping, an image from the CBERS 4A satellite was employed. Aiming to achieve higher spatial and spectral resolution for increased accuracy, the satellite sensor used corresponds to the Wide Field Imager (WFI), which has 5 spectral bands, with 4 bands at spatial resolutions of 8m and the panchromatic band at 2m. The image was obtained from the National Institute for Space Research (INPE), prioritizing a recent creation date and an image without cloud interference. Therefore, the selected image corresponds to the date of June 22, 2020.

3.2 Image Preprocessing

Procedures and geoprocessing techniques applied to images with the aim of enhancing them for use, correcting radiometric and geometric imperfections, as well as atmospheric interferences, constitute image preprocessing (BATISTA; SANTOS, 2011).

Initially, with the assistance of the QGIS software, the World Geodetic System (WGS) 84 coordinate reference system (CRS) and the Universal Transverse Mercator (UTM) projection system for zone 24 south were applied to the SRTM image and the software's workspace. Recognizing that satellite-provided images may contain inconsistent information in some pixels, the Fill sinks tool, located in the QGIS processing toolbox, was used for treatment, making it hydrologically consistent by addressing sharp depressions. Subsequently, the *r.watershed* tool from the same toolbox path was employed to extract the flow segment and drainage direction for the entire SRTM image. Utilizing the *r.water.outlet* tool, also from the same location, with the previously extracted flow and drainage data, it was possible to delineate the micro-watershed. The region was extracted in raster format, and to obtain information from it, the file was vectorized using the *r.to.vect* processing.

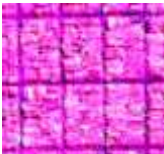


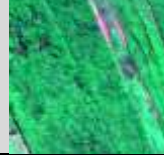



The preprocessing of the CBERS 4A image is inherent to the information previously extracted from the SRTM data. Initially, it involved applying the same CRS and projection system as was done for the SRTM Haster. Afterward, using the software tools, a composition of the 04 single bands was created, forming a multiband image with a spatial resolution of 8m. Considering that the WFI camera of the satellite provides a panchromatic band to enhance the quality of the created composition, the pan sharpening tool in QGIS was utilized, which merges the images, resulting in a spatial resolution of 2m. With this improved quality, the next steps involved clipping the image based on the previously extracted micro-watershed feature for efficiency in subsequent processes. Finally, atmospheric correction was performed using the Semi-Automatic Classification Plugin (SCP) add-on, carried out in the preprocessing area of the mentioned plugin.

3.3 Processing

To initiate the data processing stage in QGIS, the use of SCP in the Band set area was continued. Various Red-Green-Blue (RGB) compositions were created. The best-presented composition was a false-color composite using bands 431, which correspond, respectively, to near-infrared and the visible spectrum in red and blue. Additionally, the wavelength center information was entered into the SCP, a crucial detail available in the WFI camera characteristics on the INPE website. This information is of utmost importance for generating a more suitable spectral curve.

Subsequently, 7 land use and land cover classes (Table 1) were established for supervised classification. The SCP Dock panel from the SCP add-on was used to create and collect training samples. The collection of samples involves assigning various pixels to the same group, meaning that the larger the sample collection, the better the accuracy of the classification.

Table 1 – Characterization of the land use and land cover classes used.

Class	Tipologia e descrição Typology and description	Illustrative photo
1	Impervious Areas: Corresponds to areas that generate significant runoff during a precipitation event. In this class, surfaces such as asphalt, roofs, sidewalks, terraces, decks, and other impermeable areas are included.	
2	Water Bodies: Class used to gather areas of ponds, which have unique characteristics in terms of precipitation compared to other classes, and are the main areas that receive runoff. It is worth noting that this region is significant for aquifer recharge.	
3	Dense Vegetation: Class representing areas with taller trees and larger canopies than other regions. These areas are significant, as the impacts of raindrops are intercepted by the vegetation, protecting the soil and facilitating infiltration, thereby preventing excessive surface runoff.	
4	Unused/Vacant Land: Class representing areas with low vegetation in good condition, providing soil protection and reducing runoff.	
5	Livestock: Areas with vegetation in poor condition. They do not provide adequate soil protection and may result in increased runoff.	
6	Agriculture: Class representing areas used for agriculture that have reasonable potential for infiltration.	
7	Exposed Soil: Areas without any vegetation cover, susceptible to erosion. Additionally, during a rainfall event, they may result in increased runoff.	

Source: Authors (2023)

The sample collection was conducted by overlaying digital data, and associated with the color composition, the Google Satellite map base was used, covering the same period as the CBERS 4A image, from the HCMGIS add-on. This was done to observe the pixel tones representing the established classes. Accordingly, 212 collections were performed, and the data are presented in Table 2.

Table 2 – Pixels assigned by classes

Class	Description	Coletas
1	Impervious Areas	21
2	Water Bodies	17
3	Dense vegetation	29
4	Unused/Vacant Land	26
5	Livestock	47
6	Agriculture	21
7	Exposed Soil	51

Source: Authors (2023)

The classification was of the supervised type in the Band processing area of the mentioned add-on. In this stage, the MAXVER method was selected for classification.

3.4 Images post-processing

In order to obtain a more detailed analysis, additional resources available in the SCP add-on were used, specifically the Classification Reports and Accuracy tools in the Postprocessing area. The Classification Reports tool provides information on the number of pixels, area, and percentage for each created class. The Accuracy tool offers various information, including the error matrix for pixels and areas, accuracy, and the *Kappa* index.

According to Brites (1996), the Kappa index assumes that both the map obtained through classification and the reference layer created have the same degree of accuracy. As per Bishop, Feinberg, and Holland (1975), this process relates to a statistical measure, and Equation (1) shows how to calculate this index:

$$K = \frac{n \sum_{i=1}^k n_{ii} - \sum_{i=1}^k n_{i+} n_{+i}}{n^2 - \sum_{i=1}^k n_{i+} n_{+i}} \quad (1)$$

Where: k = number of rows in the error matrix; n = total number of observations (samples); n_{ii} = number of observations in row i and column i; n_{i+} = total of row i; n_{+i} = total of column i.

With the calculation of the *kappa* index, the performance of the land use and cover classification map was assessed through table 3.

Table 3 – Quality of the classification based on the Kappa coefficient.

Kappa Value	Performance
< 0,00	Poor
0,00 < k <= 0,20	Fair
0,20 < k <= 0,40	Moderate
0,40 < k <= 0,60	Good
0,60 < k <= 0,80	Very Good
0,80 < k <= 1,00	Excellent

Source: Congalton and Green (1999)

In addition, other data were obtained to verify quantitative information of the total classification and each class separately. Thus, the continuation of numerical validation processes was carried out using the error or confusion matrix, where other data such as producer's accuracy (PA), user's accuracy (UA), and overall accuracy of the map were calculated through the SCP plugin.

According to Chuvieco (1995), the overall accuracy (GA) of the map is the ratio of the elements on the main diagonal of the error matrix to the total sampled points, as shown in Equation (2).

$$GA = \frac{\sum_{i=1}^k X_{ii}}{\sum_{j=1}^k \sum_{i=1}^k X_{ij}} \quad (2)$$

Where: GA = overall accuracy; k = number of rows in the error matrix; X_{ii} = elements on the main diagonal.

The PA and UA are often understood as omission and commission errors, respectively. The former refers to incorrect determinations of the class, while the latter involves an excessive definition of the class (FERREIRA; DANTAS; MORAIS, 2007).

In general, PA can be understood as the interest that the producer has in correctly classifying a specific class or represents the probability that a particular sample represents a class on the map successfully. Thus, UA can be understood as the probability that a specific area of a class represented on the map is identified in the field (CONGALTON; GREEN, 1999).

The PA and UA were obtained for each class on the map, and Equations (3) and (4) show how these values can be calculated.

$$PA = \frac{X_{ii}}{X_{+i}} \quad (3)$$

$$UA = \frac{X_{ii}}{X_{i+}} \quad (4)$$

WHERE: X_{ii} = number of observations in i and column i; X_{i+} = total of row i; X_{+i} = total of column i.

4. Results and discussion

Despite being an urban micro-watershed, the upstream region of this area exhibits rural characteristics; the central part shows diverse land uses and occupations, while the downstream space is predominantly characterized by impermeable areas, except for Timbaúbas Park.

The supervised classification of land use and land cover in the Timbaúbas Creek micro-watershed showed that a significant portion of it is characterized as anthropized areas (Figure 3), similar to the studies by Machado *et al.* (2022) and Silva *et al.* (2022). According to Roldão *et al.* (2017), these human activities in relation to the environment are more intensified due to economic factors, leading to the prominence of pasture areas in these regions. Some areas in anthropized regions are characterized as impermeable areas, which can significantly contribute, according to Tucci (2005), to the occurrence of floods and inundations.

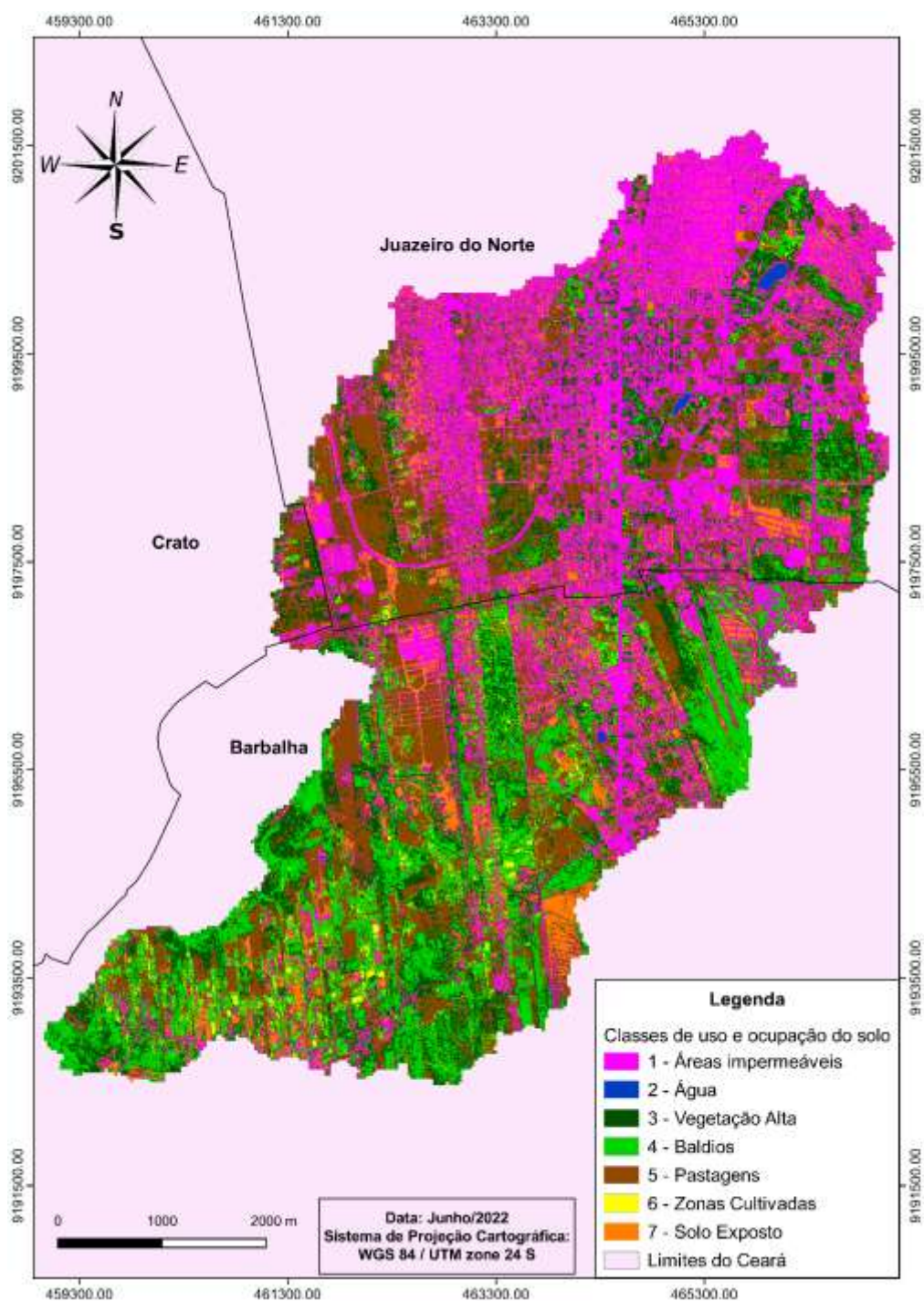


Figure 1 – Land use and land cover map of the Timbaúbas Creek micro-watershed
Source: Authors (2023)

Confusion in classification was observed between the classes of exposed soil and impermeable areas due to the reflectance of pixels. Machado *et al.* (2022) described a similar difficulty in classifying water-related areas. In the pasture, dense vegetation, and water classes, there were hardly any confusions observed in the mapping.

Class 1, corresponding to impermeable areas, accounts for 29.55% of the study area. This type of land use and cover is responsible for a significant portion of surface runoff during precipitation events, and its concentration occurs more to the north of the study area, mainly involving Timbaúbas Park.

Table 4 shows how pixel assignments occurred, the area values, and the percentage of each class in the study area.

Table 4 – Land use and land cover classification data

Class	Description	Number of Pixels	Area (m ²)	Area (%)
1	Impervious Areas	2.756.986	11.027.944	29,55
2	Water Bodies	15.142	60.568	0,16
3	Dense vegetation	1.256.415	5.025.660	13,47
4	Unused/Vacant Land	1.863.290	7.453.160	19,97
5	Livestock	1.980.726	7.922.904	21,23
6	Agriculture	266.985	1.067.940	2,86
7	Exposed Soil	1.190.601	4.762.404	12,76
Total		9.330.145	37.320.580	100,00

Source: Authors (2023)

Class 2, the water bodies class, has the lowest percentage of occupation in the analysis area, accounting for only 0.16%. In Figure 3, it is possible to observe that the distribution is punctual, with limited or concentrated presence in specific areas. On the other hand, the dense vegetation class, which is another relevant category in the region, has a significantly larger occupation, covering 13.47% of the total area. This class is broadly distributed throughout the mapped region, with a noticeable higher concentration in the southern region.

The categories of vacant lands and livestock together account for more than 40% of the mapped area. Although they are in different classes, these vegetations can alternate their concentrations depending on the time of year, meaning there may be more livestock than vacant lands at times and vice versa. Class 5 has its more concentrated zones in the western part, while class 4 predominates in the eastern and southern parts of the study area.

Agriculture constitutes the second smallest category in terms of occupation, accounting for 2.86%, equivalent to 106.79 hectares. This zone appears more intensely in the southernmost region of the study area, away from the area with the highest urban concentration, consistent with rural areas. Class 7, corresponding to exposed soil, has a significant area and is very similar in values to the dense vegetation category. This region has a 12.76% occupation, showing greater intensity in the vicinity of agriculture and impervious areas.

Regarding the data obtained from the Accuracy tool of the SCP plugin, they showed that the global accuracy value was 87.59%, and the *Kappa* coefficient of the overall map analysis corresponds to 0.84, obtaining a classification as "excellent" (Table 2). This result is close to that found by Machado *et al.* (2022) (*Kappa* coefficient of 0.82) and superior to that found by Guedes and Cestaro (2018) (*Kappa* coefficient of 0.57). The behaviors of the collected pixels can be observed in Table 5.

Table 5 – Error Matrix for Pixels

Class	1	2	3	4	5	6	7	Total
1	15.880	11	3	0	94	0	125	16.113
2	0	6.409	0	0	0	0	0	6.409
3	0	0	623	196	2	21	0	842
4	6	0	1	15.453	90	1.861	0	17.411
5	470	0	0	0	12.101	0	2	12.573
6	1	0	0	408	2	2.121	0	2.532
7	4.091	0	0	0	371	0	6.984	11.446
Total	20.448	6.420	627	16.057	12.660	4.003	7.111	67.326

Source: Authors (2023)

Table 5 shows that almost all collected pixels, intended to verify the quality of the classification for categories 2 and 3, were assigned to their respective classes, yielding satisfactory results. Out of 20,448 collected pixels for group 1, 4,091 were assigned to class 7, indicating confusion between impervious areas and exposed soil, as observed in the visual analysis.

Similarly, confusion occurred between vacant lands and agriculture, as out of 16,057 resolution units used for class 4, 408 were classified as group 6. The layer corresponding to livestock had interference with exposed soil, but it was the agriculture category that had larger areas designated incorrectly. For the 4,003 pixels selected for the study of agriculture, 1,861 were related to vacant lands. Regarding the collection for the analysis of exposed soil use and occupation, out of the 7,111 units used, 125 were identified as impervious areas.

Therefore, it can be observed that despite layers 1 and 7 causing confusion in both analyses, the more intense inconsistency is present in the verification of impervious areas. Inconsistencies between groups 4 and 6 become more pronounced when viewed from the perspective of agriculture. The possible errors regarding livestock, although they exist, can be understood as residuals from calculations or collection errors.

The quantitative and qualitative analysis of each class can be observed in Table 6. The table shows the assignments of areas for the layers, with interpretations similar to those presented in Table 5. Additionally, the values of producer accuracy, user accuracy, and *Kappa* coefficient for each category are provided, calculated by the SCP plugin based on the relative area.

Table 6 – Error Matrix for Land Cover Classification and Analysis Data

Class	Relative Area							Total
	1	2	3	4	5	6	7	
1	0,29120	0,00020	0,00010	0,00000	0,00170	0,00000	0,00230	0,29550
2	0,00000	0,00160	0,00000	0,00000	0,00000	0,00000	0,00000	0,00160
3	0,00000	0,00000	0,09960	0,03130	0,00030	0,00340	0,00000	0,13470
4	0,00010	0,00000	0,00000	0,17720	0,00100	0,02130	0,00000	0,19970
5	0,00790	0,00000	0,00000	0,00000	0,20430	0,00000	0,00000	0,21230
6	0,00000	0,00000	0,00000	0,00460	0,00000	0,02400	0,00000	0,02860
7	0,04560	0,00000	0,00000	0,00000	0,00410	0,00000	0,07790	0,12760
Total	0,34480	0,00180	0,09970	0,21320	0,21160	0,04870	0,08020	1,00000
Area (m ²)	12.869.804	68.097	3.720.992	7.956.949	7.895.479	1.816.574	2.992.686	37.320.580
PA (%)	84,45	88,94	99,93	83,13	96,58	49,25	97,10	
UA (%)	98,55	100,00	73,99	88,75	96,25	83,77	61,02	
Kappa	0,98	1,00	0,71	0,86	0,95	0,83	0,58	

Source: Authors (2023)

With the *Kappa* coefficient values for each class shown in Table 6, it is evident that class 7 is the group with the lowest value (0.58), and according to Table 3, this category is classified as having "Good" performance, following Congalton and Green (1999). Similarly, class 3 is designated as "Very Good," while the others (1, 2, 4, 5, and 6) are considered classes that had their processing classified as "Excellent."

The UA values show the same agreement as presented by the *Kappa* index and exhibit variations concerning the PA. According to Table 6, classes 4 and 5 have small variations regarding user and producer accuracy. In contrast, categories 6 and 7 show the greatest divergence in these results. It is still possible to observe that groups 3, 5, and 7 are more likely to have their samples correctly identified by the user than the probability of these classes presented in the mapping to be genuinely recognized in the field. The opposite occurs with the interpretation of classes 1, 2, 4, and 6, as they have a higher UA than the PA.

5. Conclusions

The high spatial resolution image, formed through the fusion of CBERS 4A satellite bands and the use of QGIS SCP, enabled mapping of land use and cover that is consistent with Google Satellite images. Despite being a supervised classification, where the user plays an essential role, the use of satellite images for comparative analysis with mapping becomes an effective alternative when access to the location is challenging, as in the case of remote regions in the semi-arid areas where there are typically no access roads.

The use of high-quality imagery for mapping proved sufficient to distinguish various types of land use and cover, and visual inspection becomes essential to analyze the image classification. However, constructing an error matrix of pixel and area assignments is necessary to understand the limitations of a semi-automatic mapping; it is also crucial for using the data with greater confidence. Statistical studies to assess the performance of the overall analysis, and consequently, the categories, provide a way to analyze quantitatively and qualitatively how the map processing occurred.

The use of producer accuracy and user accuracy in the quantitative analysis of mapping provides data on omission and commission errors that can confirm the acceptance of the processing or indicate a reclassification of the image. These results also show where the confusion of pixel assignments is occurring and the probability of finding a particular class on the map and confirming it in the field. Thus, the use of PA and UA is an efficient way to numerically observe how the classification of classes occurred.

The land use and land cover map showed satisfactory and consistent results, facilitating its use to determine the runoff coefficient. This factor is of utmost importance to understand the volume of surface water runoff during a design rain, which can be used for sizing hydraulic equipment to prevent flooding and advances in erosive processes. Thus, this information can provide data that contribute to applications in the field of water resources, the environment, and various other areas of interest.

References

- ALEXANDRE, F. da S. Land Use Mapping in the Municipality of Palmeirina-PE. *Northeast Geosciences Journal*. [S. l.], vol. 2, p. 1160–1167, 2016.
- Alexandre et al. Geoprocessing and Remote Sensing Applied in the Survey and Mapping of Vegetal Degradation between 1987 and 2010 in the Municipality of Iati-P. *Rev. Geoscience. Northeast*, Vol.2, (2016b). Special Edition.
- BATISTA, J. L. O.; SANTOS, R. L. Analysis of the Dynamics of Land Use and Occupation in Small Semi-Arid Municipalities of Bahia: The Case of Teofilândia. *North Grande Geography Journal*, no. 49, Santiago, 2011.
- BANDEIRA, A. P. N.; MACEDO, C. C. A.; CLARINDO, G. S.; LIMA, M. G. S.; SOUZA NETO, J. B. Assessment of Potential Surface Degradation Resulting from Erosion Processes in Environmentally Protected Area. *SOILS & ROCKS JCR*, vol. 44, p. 1-10, 2021.
- BISHOP, Y. M.; FEINBERG, S. E.; HOLLAND, P. W. *Discrete Multivariate Analysis - Theory and Practice*. Cambridge, 1975.
- BRAGA, G. N. M. *Soil Fertility and Pasture Management to Recover Degraded Pastures*. Available at: <https://agronomiacomgismonti.blogspot.com/2013/05/fertilidade-do-solo-e-manejo-do-pasto.html>. Accessed on: May 15, 2022.
- BRITES, R.S. *Accuracy Verification in Orbital Digital Image Classification: Effect of Different Sampling Strategies and Evaluation of Accuracy Indices*. Viçosa, 1996. Doctoral Thesis (Forestry Science) - Federal University of Viçosa.
- Caldeira, C. R. T. et al. Comparison between Digital Terrain Models Generated by P-band Radar and LiDAR in the Amazon, a Case Study in Amapá (Brazil). *Rev. Geoscience. Northeast*, Caicó, vol.9, no.1, (Jan-Jun) p.59-70, 2023.
- CHUVIECCO, E. *Fundamentals of Space Remote Sensing*. Madrid, Spain. Rialp Editions, 1995.
- CONGALTON, R.G.; GREEN, K. *Assessing the Accuracy of Remotely Sensed Data: Principles and Practices*. New York, Boca Raton: Lewis Publishers, 1999.

- FERREIRA, E.; DANTAS, A.A.A.; MORAIS, A.R. Accuracy in the Classification of Forest Fragments in Cbers-CCD Satellite Image, in the Municipality of Lavras, MG. In: XIII Brazilian Symposium on Remote Sensing, 2007, Florianópolis, SC, Brazil. Proceedings.. Florianópolis: INPE/SELPER Brazil, 2007, p. 887-894.
- FITZ, P. R. Geoprocessing without Complication. 3rd ed. revised and expanded. São Paulo. 2013. 26p.
- G1 CENTRO-OESTE DE MINAS. Owners of Dirty Properties, Lands, and Lots Have Up to 30 Days to Clean Sites in Arcos. February 24, 2021. Available at: <https://g1.globo.com/mg/centro-oeste/noticia/2021/02/24/donos-de-imoveis-terrenos-e-lotessujos-tem-ate-30-dias-para-limpar-locais-em-arcos.ghtml>. Accessed on: May 22, 2022.
- GALO, M.L.B.T.et al. Use of Orbital Remote Sensing in Monitoring the Dispersion of Macrophytes in the Reservoirs of the Tietê Complex. Weed Plant, Viçosa-MG, *Northeast Geosciences Journal*, vol.20, p.7-20, 2002. Special Edition.
- GUEDES, J.C. F; CESTARO, L. A. Strategy for Accuracy of Land Cover Maps in the Brazilian Semi-Arid: Case Study in the Municipality of Martins/RN. *Northeast Geosciences Journal*, Vol. 4, Special Issue (2018)
- HARADA, K. Urban Area and Urban Expansion Area. May 2018. Available at: <https://genjuridico.jusbrasil.com.br/artigos/605579098/area-urbana-e-area-de-expansao-urbana>. Accessed on: May 15, 2022.
- IPECE - INSTITUTE OF RESEARCH AND ECONOMIC STRATEGY OF CEARÁ. Municipal Profile – 2017 - Juazeiro do Norte, 2017.
- LIMA, S. M.; SOUZA, J. O. P., Detailing of Soil Classes in the Watershed of Riacho do Tigre. *Northeast Geosciences Journal*, Vol.2, p 103-112, (2016). Special Edition.
- Machado et al. Geoprocessing Applied to the Environmental Area: a Case Study Based on Digital Image Processing and Remote Sensing. *Brazilian Journal of Development*, Curitiba, vol.8, no.4, p.23819-23836, Apr., 2022.
- ROLDÃO, A. F.; PETRUCCI, E.; CASTRO, F. S. Analysis of Land Use and Occupation in the Córrego Água Vermelha Basin, Municipality of Uberlândia-MG, Through Free Software Qgis. In: Brazilian Symposium of Applied Physical Geography, 17., 2017.
- PEREIRA, C. M. C. Socio-Environmental Analysis of the City of Juazeiro do Norte: Subsidies for the Construction of the Local Agenda 21. 2013. Doctoral Thesis, Institute of Geosciences and Exact Sciences, Rio Claro – SP, 2013.
- SANTOS, C. L. dos. IMPACTS OF URBANIZATION ON WATERSHEDS: THE CASE OF THE JAGUARIBE RIVER BASIN, CITY OF JOÃO PESSOA/PB. *Northeast Geosciences Journal*, [S. 1.], vol. 2, p. 1025–1033, 2016. DOI: 10.21680/2447-3359.2016v2n0ID10565. Available at: <https://periodicos.ufrn.br/revistadoregne/article/view/10565>. Accessed on: July 29, 2023.
- Silva et al. Use of Remote Sensing for Calculation of Use and Occupation in Córrego do Grotão, Capitólio – Minas Gerais. *Journal of Sciences and Innovation*, Rio Grande do Sul, vol. 09, 2023.
- SILVA, P. L. F.; SILVA, A. J. Evaluation of Land Use and Occupation in the Municipality of Pilõesinhos-PB, from 1984-2016 using Geoprocessing. *Rev. Geoscience. Northeast*, Vol. 3, No. 1 (2017).
- SOUSA, R. dos S. Evaluation of Vegetation Cover and Land Use in the Coastal Watershed of the Portinho River, Piauí. *Northeast Geosciences Journal*, [S. 1.], vol. 2, p. 1141–1150, 2016.
- TATUAPÉ. Tatuapé More Green: Parks and Vegetation of the Neighborhood are Part of the Urban Forest. June 23, 2016. Available at: <https://alotatuape.com.br/tatuape-mais-verdeparques-e-vegetacao-do-bairro-fazem-parte-da-floresta-urbana/>. Accessed on: May 15, 2022.
- TRIPADVISOR. Nature, Exuberance, and Urban Planning. February 16, 2020. Available at: https://www.tripadvisor.com.br/ShowUserReviews-g312741-d480841-r745461248-Lagos_de_Palermo-Buenos_Aires_Capital_Federal_District.html. Accessed on: May 22, 2022.

TUCCI, C. E. M. *Urban Rainwater Management*– Ministry of Cities – Global Water Partnership - World Bank – Unesco 2005.

TUCCI, Carlos E. M. **Hydrology: Science and Application**. Porto Alegre: University Publisher/UFRGS, ABRH: EDUSP, 1993.